Flattening the Polarization Energy Landscape in $BiFeO_3$-Based Dielectrics via Nanoscale Phase Coexistence for Superior Electrostatic Energy Storage

Jiarong Lv[1], Dingheng Lin[1], Ya Yang[1], Wei Zhang[1], Sen Chen[1], Jinjun Liu[1]*, Ning Liu[2]*, Huajie Luo[3], and Zhongbin Pan[1]*

[1]School of Materials Science and Chemical Engineering, Ningbo University, Ningbo, Zhejiang, 315211, China. E-mail: panzhongbin@163.com (Z. Pan), liujinjun1@nbu.edu.cn (J. Liu)

[2]Engineering & Technology Center for Aerospace Materials, Wuzhen Laboratory of Tsinghua University, 925 Daole Road, Jiaxing 314500, China. E-mail: liun@wuzhenlab.com (N. Liu)

[3]School of Materials Science and Engineering, University of Science and Technology Beijing, Beijing 100083, China

Experimental section

Ceramic synthesis: Lead-free ceramics with compositions of $Bi_{0.85}Sm_{0.15}FeO_3$ and (1-x)$Bi_{0.85}Sm_{0.15}FeO_3$-x(0.965$Ba_{0.6}Sr_{0.1}Bi_{0.2}TiO_3-0.035BiMg_{0.5}Zr_{0.5}O_3$) (where x = 0.4, 0.5, 0.6, and 0.7) were prepared via a conventional solid-state reaction route. High-purity powders including Bi_2O_3 (99%), Sm_2O_3 (99.9%), Fe_2O_3 (99%), $BaCO_3$ (99.8%), $SrCO_3$ (99%), TiO_2 (99%), MgO (98%), ZrO_2 (99%), and MnO_2 (99.95%) were used as starting materials. These powders were weighed according to stoichiometric proportions, mixed thoroughly in ethanol, and subjected to ball-milling for 12 hours using ZrO_2 grinding media. After drying completely, the mixed powders were calcined at 800 °C for 3 hours with the addition of 0.1 *wt*% MnO_2 as a sintering aid. The resulting powder was then pressed into discs with a radius of 1 cm and sintered at temperatures ranging from 1040 to 1080 °C for 3 hours, following the removal of polyvinyl alcohol (PVA) at 500 °C. The obtained ceramic samples were carefully polished to a thickness of 40–50 μm, and gold electrodes with a radius of 1 mm were deposited on both sides for subsequent electrical measurements.

Characterization: The ceramic phase structure was analyzed by XRD (PANalytical Empyrean, 10°min^{-1}, 20°-80°). Raman spectroscopy (Renishaw inVia) was employed to investigate the influence of doping on the local chemical structure. The domain configuration and the corresponding SAED mapping were performed on a JEOL JEM-2100F microscope. Atomic-scale HAADF imaging was performed on Cs-corrected JEOL JEM-ARM300F and Hitachi HF5000 microscopes. The surface morphology of the samples was observed using a scanning electron microscope (SEM, Regulus 8230). The sintered ceramic samples were polished to a final thickness of approximately 40-50 μm. Circular gold electrodes with a diameter of 2 mm were deposited on both surfaces of the samples via sputtering. Polarization-electric field (*P*-*E*) hysteresis loops were measured at room temperature using a

ferroelectric test system (TF Analyzer 2000) under unipolar electric field excitation at a frequency of 100 Hz. Fatigue resistance was evaluated over 1-10,000 cycles, while frequency-dependent (1-120 Hz) and temperature-dependent (20-140 °C) stability assessments were also conducted. The temperature dependence of the dielectric properties was measured from 20 °C to 500 °C across a frequency range of 1 kHz to 1000 kHz using an LCR meter (TH2838A). Charge–discharge behavior was characterized under a resistive-inductive load circuit (SDS5032X) with a load resistance of 150 Ω.

Phase-field simulation

A scalar damage field, $s(x,t)$ is introduced as the order parameter to characterize the dielectric breakdown process of ceramics by analogy with mechanical fracture. The value of (s) varies from 0 to 1, with (s = 1) corresponding to the intact insulating state and (s = 0) corresponding to the fully damaged conductive state. Upon complete breakdown, the ceramic material loses its insulating capability and forms a conductive breakdown channel. For numerical simplicity, the fully damaged phase is regarded as a dielectric phase with a large but finite dielectric constant of (ε_0/η), where (ε_0) is the initial dielectric constant of the intact phase and (η) is a sufficiently small positive parameter. For partially damaged intermediate states, the dielectric constant is interpolated as follows:

$$\varepsilon(s) = \frac{\varepsilon^0}{f(s) + \eta'} \qquad \text{Eq. S1}$$

where $f(s)=4s^3-3s^4$, the ratio of ε_g to ε_{gb} is set as 10:1 in this work generally. If the process reduces the total potential energy of the system, breakdown,

$$\prod[s,\phi] = \int_{\Omega} \left[\hat{W}_{es}(E,s) + W_d(s) + W_i(\nabla s)\right] dV \qquad \text{Eq. S2}$$

where $\hat{W}_{es}(E,s) = -\frac{\varepsilon}{2}E \cdot E$ is the electrostatic residual energy per unit volume, $W_d(s) = W_c[1 - f(s)]$ is the breakdown energy function, and W_c represents the critical electrostatic energy density required for the formation of the damaged phase. $W_i(\nabla s) = \frac{\Gamma}{4}\nabla s \cdot \nabla s$ is the gradient energy term, which is introduced to regulate the sharpness of the phase boundary between the intact and damaged regions. It should be noted that the material parameter Γ is approximately related to the breakdown energy. According to the linear kinetic law, $\partial s/\partial t = -m\delta \prod/ \delta s$, substituting the specific form of the energy function gives the evolution equation for the breakdown variable:

$$\frac{1\partial s}{m\partial t} = \frac{\varepsilon'(s)}{2}\nabla\phi \cdot \nabla\phi + W_c f'(s) + \frac{\Gamma}{2}\nabla^2 s \qquad \text{Eq. S3}$$

the mobility coefficient m controls how fast the damaged region develops once the local electrostatic driving force reaches the breakdown criterion. To simplify the numerical implementation and make the governing equation independent of specific dimensional units, all variables were converted into dimensionless quantities. Specifically, the spatial coordinate was scaled by the characteristic breakdown length (l), the energy density was scaled by the critical breakdown energy density (W_c), the time was scaled by the characteristic time (t_0), and the electric potential was scaled by $\sqrt{\Gamma/\varepsilon^0}$. After this normalization treatment, the evolution equation for the damage field can be written in dimensionless form as follows:

$$\bar{\nabla} \cdot \left[\frac{1}{f(s) + \eta}\bar{\nabla}\bar{\phi}\right] = 0 \qquad \text{Eq. S4}$$

$$\frac{\partial s}{\partial t} = -\frac{f'(s)}{2[f(s)+\eta]^2}\bar{\nabla}\bar{\phi}\cdot\bar{\nabla}\bar{\phi} + f'(s) + \frac{1}{2}\bar{\nabla}^2 s \qquad \text{Eq. S5}$$

In the normalized formulation, overbars are used to distinguish dimensionless quantities from their dimensional counterparts. The resulting equations were solved in *COMSOL* Multiphysics to capture the progressive formation of breakdown paths within the ceramic. Instead of directly imposing a fixed voltage, the external electrical load was increased quasi-statically by adjusting the amount of charge on the negative electrode, which generated the corresponding potential difference across the two electrodes.

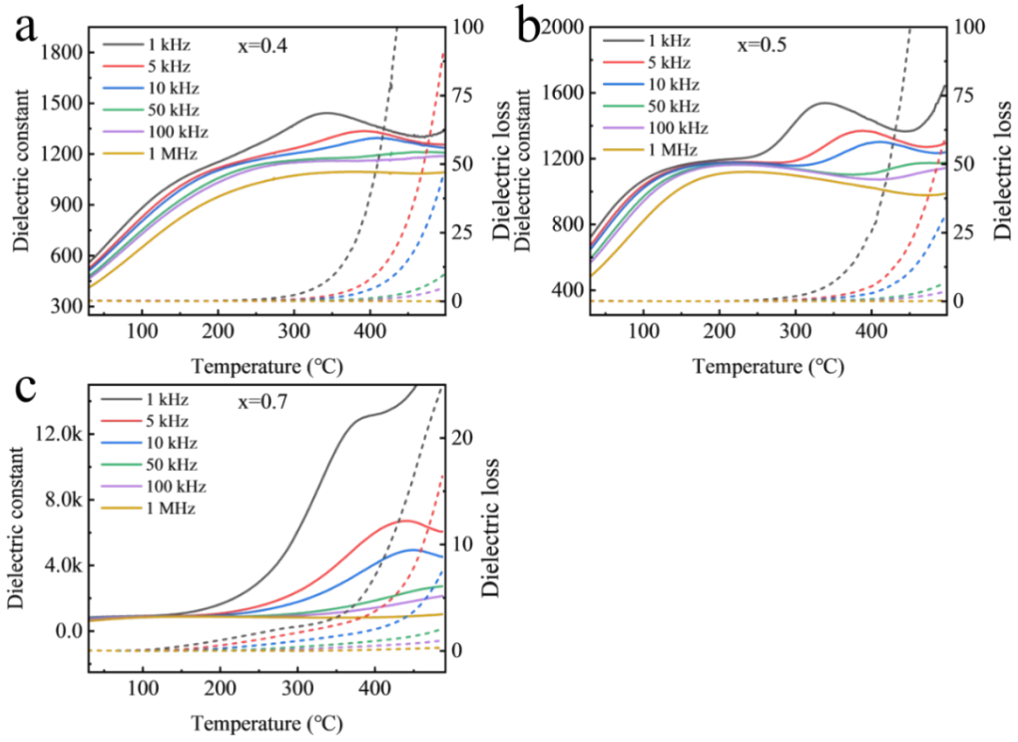

Figure S1. Temperature-related dielectric constants and loss of (a) pristine x=0.4, (b) x=0.5, and (c) x=0.7.

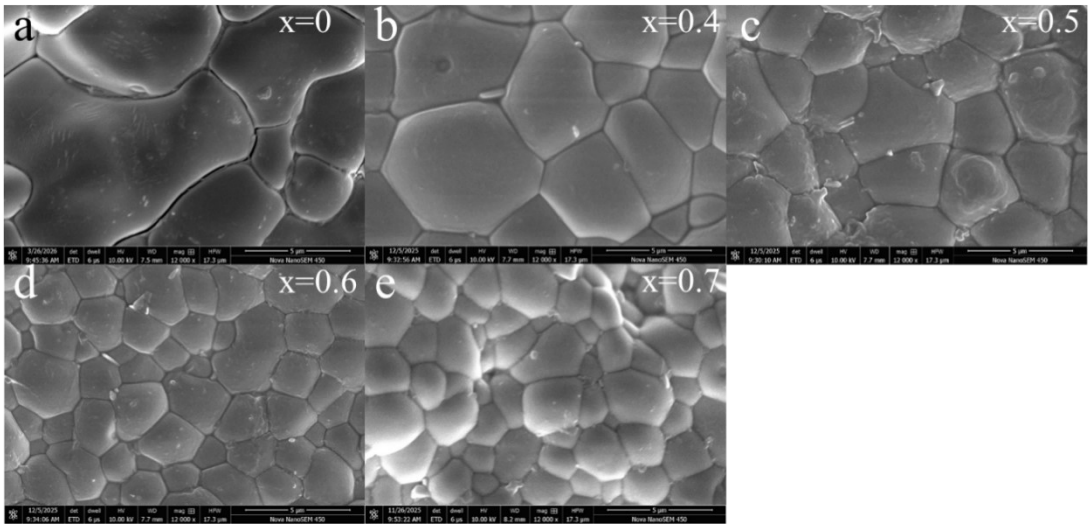

Figure S2. SEM images of (a) x=0, (b) x=0.4, (c) x=0.5, (d) x=0.6, and (e) x=0.7 ceramics.

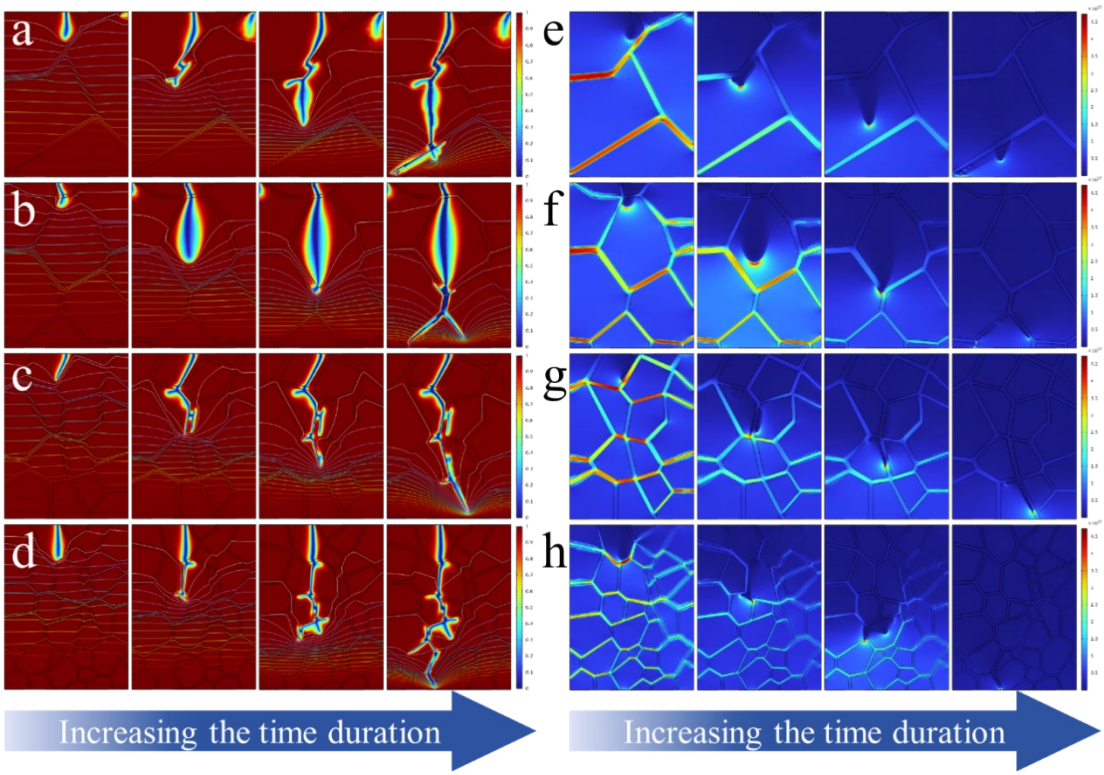

Figure S3. Breakdown paths of (a) x=0, (b) x=0.4, (c) x=0.5, and (d) x=0.7 ceramics and local electric field distribution of (e) x=0, (f) x=0.4, (g) x=0.5, and (h) x=0.7 ceramics under phase field simulation.

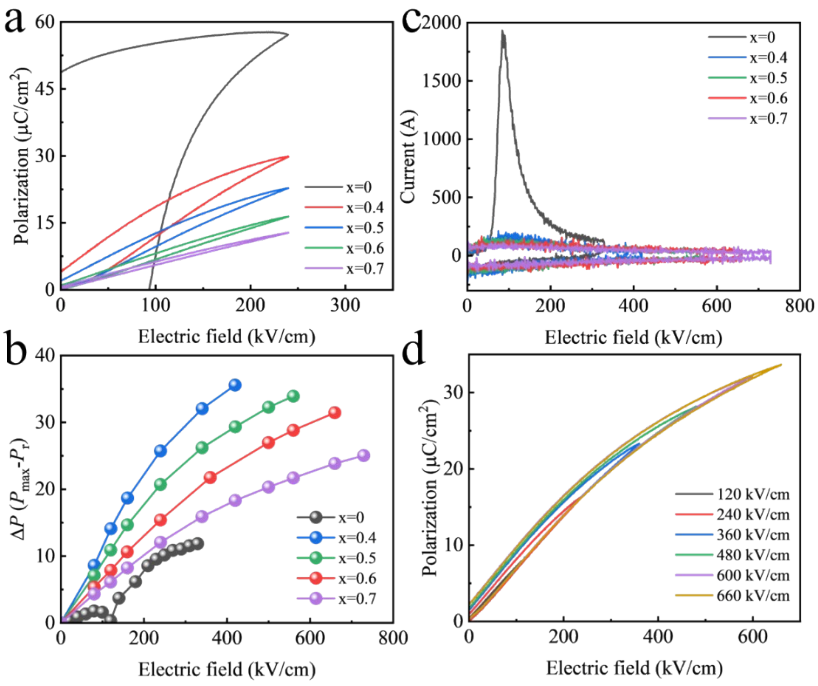

Figure S4. (a) The *P*-*E* loops of BSF-x(BSBT-BMZ) ceramics under low electric field. (b) The Δ*P* (P_{max}-P_r) of BSF-x(BSBT-BMZ) ceramics as functions of the applied electric field. (c) The *I*-*E* loops of BSF-x(BSBT-BMZ) ceramics under the critical breakdown electric field. (d) *P*-*E* loops measured with different applied electric fields of BSF-0.6(BSBT-BMZ) ceramic.

Table S1. Vogel–Fulcher fitting parameters of different compositions.

Composition	T_0/K	E_a/eV	v_0/Hz
x=0	484.7148	0.02986	8.00038E6
x=0.4	374.12931	0.03964	1.26387E7
x=0.5	333.75214	0.05321	7.09378E7
x=0.6	295.09214	0.07351	7.68579E8
x=0.7	262.23892	0.08655	2.59713E9